Topology optimization of plate structures for sound transmission loss improvement in specific frequency bands

Daniele Giannini[1], Mattias Schevenels[2], Edwin Reynders[1]

[1] Department of Civil Engineering - Structural Mechanics Section, KU Leuven, Leuven, Belgium.
daniele.giannini@kuleuven.be, edwin.reynders@kuleuven.be
[2] Department of Architecture - Architectural Engineering Section, KU Leuven, Leuven, Belgium.
mattias.schevenels@kuleuven.be

Abstract
In the design of plate structures it is of particular interest to bound the levels of sound transmission and related discomfort. In presence of narrowband excitations, such as harmonic loads due to rotating machines, a reduced sound transmission can be achieved through a limited mechanical response by avoiding structural resonances in the related frequency bands. This also helps in preserving the structural integrity. In this work, an approach based on topology optimization is proposed to find the optimal material thickness distribution within the plate area, in order to maximize the width of the frequency band that does not contain structural eigenfrequencies. The method is here applied targeting different frequencies in the audible range and focusing on practically relevant design cases, such as the optimal design of PMMA panels and single glazing structures. An efficient optimization is obtained through a simple mechanical Finite Element (FE) model to predict the structural eigenfrequencies, and the improvement in Sound Transmission Loss (TL) for the optimized designs is then verified through hybrid Finite Element-Statistical Energy Analysis (FE-SEA) simulations.

Keywords: Topology optimization, sound transmission loss, optimal material distribution, PMMA panel, glazing panel.

1   Introduction

In the design of plate structures, improved vibration response and sound insulation behaviour in specific frequency bands can be achieved by considering a non-uniform material distribution [1,2]. An interesting approach is to design optimal structures with controlled eigenfrequencies, as eigenfrequencies are the key elements in obtaining the desired dynamic vibroacoustic performance [1] and can be computed with reduced computational cost with respect to full dynamic simulations for several frequencies.

In presence of narrowband disturbances, such as harmonic loads due to rotating machines, the vibroacoustic performance of the structure can be improved by moving its eigenfrequencies as far as possible from the disturbance frequency. In this paper, we apply this design strategy to plate panels for civil applications, in order to effectively bound the levels of vibration and sound transmission, i.e. preserving the structural integrity while improving the comfort of people. The focus is on both PMMA and glazing panels, that will be optimized considering different possible disturbance frequencies in an application relevant range.

The design problem is solved through the topology optimization approach [3], in order to find the optimal thickness distribution within the panel area that maximizes the width of the frequency band around the disturbance that has no eigenfrequencies. The optimal layouts are found relying on an in-vacuo mechanical finite element model of a simply supported plate, that allows for a computationally efficient optimization. The sound insulation performance of the optimized layouts are verified a posteriori through a hybrid finite element statistical energy analysis (FE-SEA) model [4], in which the deterministic (FE) model of the plate is coupled with the sound fields in the source and receiving rooms, modelled as diffuse (SEA) subsystems.

The present paper is organized as follows: Section 2 describes the mechanical finite element model used to compute the structural eigenfrequencies, along with the considered design variables to describe the thickness

distribution. Section 3 presents the formulation of the topology optimization problem and the details of the associated solution procedure. The results of the topology optimization when optimizing the modal behaviour of the panel are shown in Section 4, while in Section 5 we verify the achieved improvements on the sound transmission loss by hybrid FE-SEA analyses. Finally, Section 6 concludes the paper with a summary of the main findings and drawing the related conclusions.

2   Mechanical finite element model of the plate and design variables

Referring to Figure 1, the plate panel is modelled as simply supported on its four edges, and discretized by 50 $\times$ 50 Kirchhoff plate elements. The eigenfrequencies ω_i and the modal shapes $\mathbf{\Phi_i}$ of the structure can be found by solving the following eigenvalue problem:

$$\left(\omega_i^2 \mathbf{M} + \mathbf{K}\right)\mathbf{\Phi_i} = \mathbf{0} \tag{1}$$

where $\mathbf{K}$ and $\mathbf{M}$ are the global stiffness and mass matrices respectively. The eigenfrequencies in Hz can be found as $f_i = \omega_i/2\pi$.

The thickness distribution is described by associating each e-th finite element with a design variable $\gamma_e \in [0,1]$ that is used to scale the element thickness. The filtering scheme from [5] is applied to the field of design variables $\mathbf{\gamma}$, in order to avoid spurious checkerboard layouts and mesh dependence in the obtained solution. Starting from γ_e, the filtered design variables are obtained through the following convolution type filter:

$$\tilde{\gamma}_e = \frac{\sum_{j \in \mathbb{N}_{s,e}} w(\mathbf{x_j}) v_j \gamma_{e,j}}{\sum_{j \in \mathbb{N}_{s,e}} w(\mathbf{x_j}) v_j} \tag{2}$$

where v_j is the volume of the j-th element and $\mathbb{N}_{s,e}$ is the set of neighbouring elements, i.e. the set of elements lying within a circle with radius r_{min} centred on the centroid of element e. The linear weighting function $w(x_j)$ is given as:

$$w(\mathbf{x_j}) = r_{min} - |\mathbf{x_j} - \mathbf{x_e}| \tag{3}$$

where $\mathbf{x_j} = (x_j, y_j)$ and $\mathbf{x_e} = (x_e, y_e)$ are the coordinates of the centroids of elements j and e.

The filtered design variables are used to scale the thickness of each finite element between a minimum and a maximum value (t_{min} and t_{max} respectively), and then to accordingly scale its stiffness and mass matrices:

$$t_e = t_{min} + (t_{max} - t_{min}) \cdot \tilde{\gamma}_e \quad \Rightarrow \quad \mathbf{K}_e(t_e) = \mathbf{K}_e(t=1) \cdot t_e^3, \quad \mathbf{M}_e(t_e) = \mathbf{M}_e(t=1) \cdot t_e \tag{4}$$

where $\mathbf{K}_e(t=1)$ and $\mathbf{M}_e(t=1)$ are the matrices related to reference elements with unitary thickness. The scaled element matrices are assembled to find the global matrices used in Eq. (1).
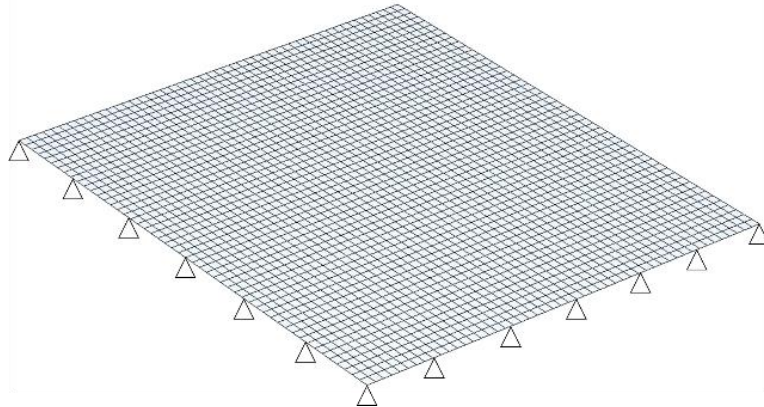
Figure 1 – Scheme of a simply supported plate discretized by finite elements.

3   Formulation and solution of the topology optimization problem

The design problem is formulated in order to find the optimal thickness distribution within the panel area, that maximizes the width of the frequency band with no structural eigenfrequencies around the disturbance frequency. This is achieved by considering the following objective function and constraints:

$$\max_{\gamma,\beta} \beta$$
$$\text{subject to:} \begin{cases} \beta \leq \dfrac{|f_i - f_c|}{f_c} & \forall i \\ \text{Vol} = \dfrac{\sum_e v_e \tilde{\gamma}_e}{\sum_e v_e} \leq 1 \end{cases} \tag{5}$$

Referring to Figure 2, the focus is on the normalized distance $|f_i - f_c|/f_c$ between the i-th eigenfrequency f_i and the disturbance frequency f_c. In order to maximize the normalized distance of the closest eigenfrequency, we introduce a further design variable β, that is used as the objective function to be maximized while imposing that β is lower than all the considered normalized distances. As it will be shown in the next Section, the final value of the objective function β will be therefore directly related to the width of the obtained frequency range with no eigenfrequencies. No particular constraints are imposed on the fraction of usable material Vol, that is free to vary between 0 and 1.

The formulated optimization problem in Eq. (5) is solved for local optimality using the gradient-based Method of Moving Asymptotes (MMA) [6]. The method iteratively updates the thickness distribution depending on the values and the derivatives of objective function and constraints, until all constraints are satisfied and a maximum in the objective function is found. In particular, the sensitivities of objective function and constraints are found analytically, by differentiating their expressions and by exploiting the expression for eigenvalue sensitivities found in [3].

We note that our preliminary numerical experiments have shown that the considered design problem results to be non-convex, and the local optimum found by the MMA in general depends on the initial set of design variables. In order to mitigate this effect and better approximate the global optimum, we therefore perform multiple optimizations for each considered design case, by considering different initial guesses consisting of uniform thickness distributions with different constant values.
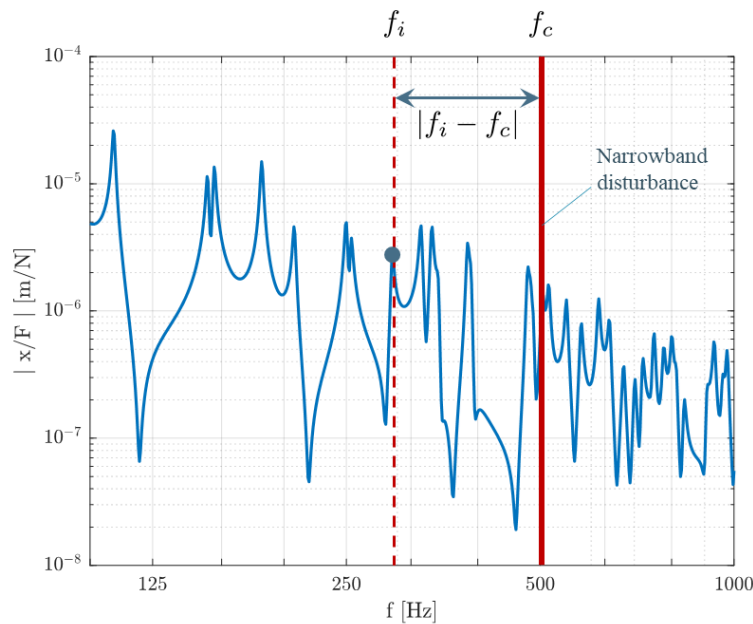
Figure 2 – Illustrative mechanical response of a plate panel, with marked distance between the disturbance frequency f_c and the i-th eigenfrequency f_i.

Table 1 – Material and geometrical properties of the considered PMMA and glazing panels.

	ρ [kg/m^3]	E [GPa]	ν	η	Panel dimensions	t_{min} [mm]	t_{max} [mm]
PMMA	1275	4.5	0.35	0.06	1 m × 1 m	15	60
Glazing	2500	62	0.22	0.01	1.25 m × 1.25 m	4	12

The design targets practical applications related to single PMMA and glazing panels, that due to the varying thickness will be translucent but not fully transparent. The considered material parameters (mass density ρ, Young modulus E, Poisson ration ν, damping loss factor η), along with the panel dimensions and the range of variation $[t_{min}, t_{max}]$ for the thickness are listed in Table 1.

4 Optimization results: designed layouts

The optimized layouts for PMMA and glazing panels are shown in Figures 3 and 4 respectively, while the corresponding values of the objective function β are listed in Tables 2 and 3. As previously mentioned, β directly relates to the width of the obtained frequency band with no eigenfrequencies: in the Tables also its reference values for 1/3-octave and octave bands are reported. Different disturbance frequencies f_c have been considered for the designs, all in a relevant range for practical applications between 125 and 2000 Hz.

The optimized layouts show how the algorithm is able to effectively modulate the thickness within the panel area, in order to properly tailor the stiffness and mass distributions and control the eigenfrequencies of the system. In particular, we see how the complexity in the geometric features described by the thickness distribution increases at higher target disturbance frequencies, as higher order modes need to be controlled with a more detailed modulation of the panel properties.

Also, we see how the relative width of the obtained frequency band with no eigenfrequencies decreases as the target disturbance frequency increases: at higher frequencies, the frequency bands (i.e. 1/3-octave bands and octave bands) become wider, and therefore they involve a higher number of modes to be controlled. Even if this makes it more difficult to obtain a wide frequency band with no eigenfrequencies, for all the presented design cases at least around a 1/3-octave band with no eigenfrequencies around the disturbance has been obtained.
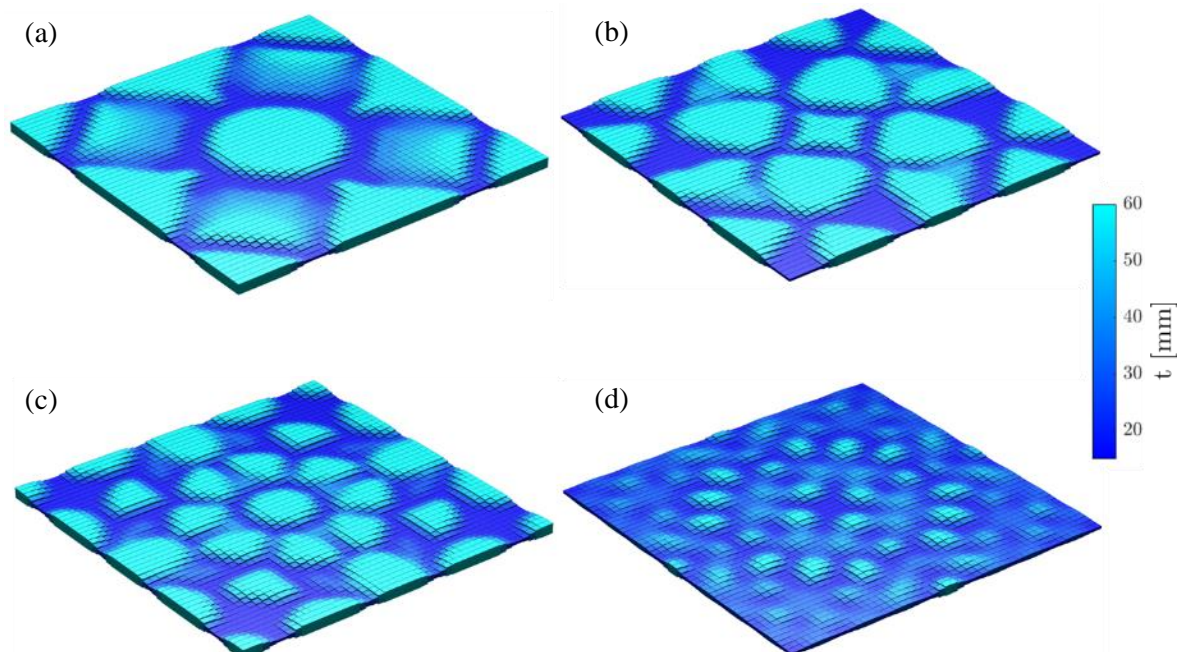
Figure 3 – Optimized layouts for the PMMA panel: (a) $f_c = 250\ Hz$, (b) $f_c = 500\ Hz$, (c) $f_c = 1000\ Hz$, (d) $f_c = 2000\ Hz$.

Table 2 – Objective functions for the PMMA optimized layouts in Figure 3

Layout	(a) $f_c = 250$ Hz	(b) $f_c = 500$ Hz	(c) $f_c = 1000$ Hz	(d) $f_c = 2000$ Hz
β(*)	0.429	0.323	0.227	0.120

(*) $\beta = 0.1225$: 1/3-octave band with no eigenfrequencies, $\beta = 0.4142$: octave band with no eigenfrequencies
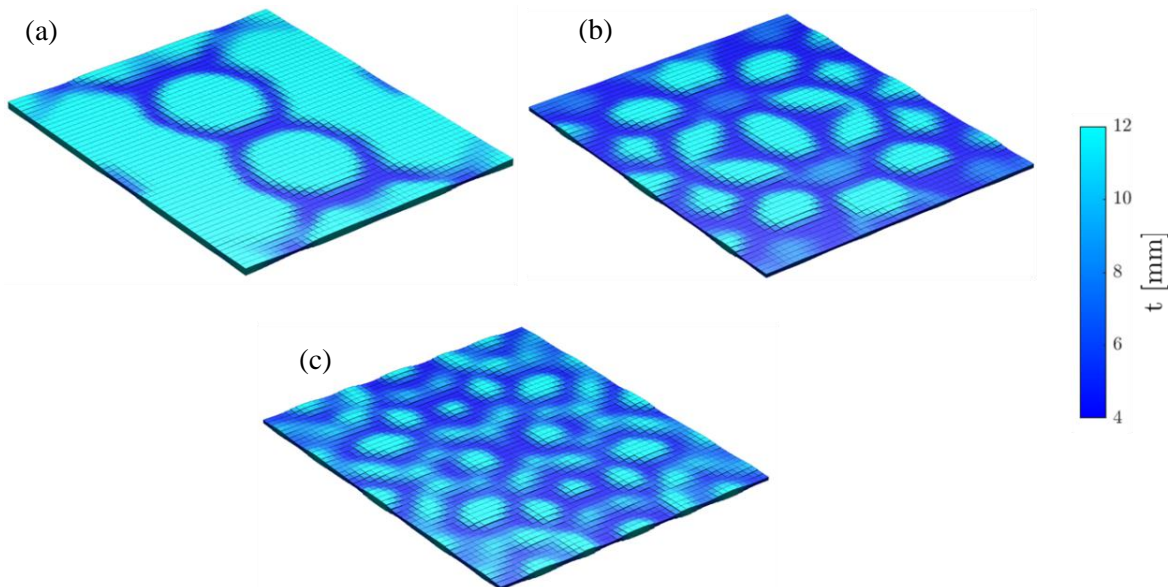
Figure 4 – Optimized layouts for the glazing panel: (a) $f_c = 125$ Hz, (b) $f_c = 250$ Hz, (c) $f_c = 500$ Hz.

Table 3 – Objective functions for the glazing optimized layouts in Figure 4

Layout	(a) $f_c = 125$ Hz	(b) $f_c = 250$ Hz	(c) $f_c = 500$ Hz
β(*)	0.278	0.207	0.138

(*) $\beta = 0.1225$: 1/3-octave band with no eigenfrequencies, $\beta = 0.4142$: octave band with no eigenfrequencies

5 Sound transmission loss computation through the FE-SEA model

Pushing eigenfrequencies away from the disturbance reduces the vibration response of the structure and therefore is effective in preserving the structural integrity. In the following we will also verify how this considered design objective allows to improve the sound insulation behaviour.

The performances of the optimized layouts in terms of sound transmission loss (TL) are computed through the hybrid FE-SEA (Finite Element – Statistical Energy Analysis) modelling framework [4,7]: in this case the plate is modelled deterministically through finite elements to capture its vibration behaviour in full detail, while the sound fields in the source and receiving rooms are modelled as diffuse (SEA) subsystems. The diffuse sound fields in the transmission rooms and the deterministic plate model are coupled by employing the diffuse field reciprocity relationship [8], resulting in a full transmission suite (room-wall-room) model [4,9,10].

The sound transmission loss is computed as $TL = 10 \log 1/\tau$, where the sound transmission coefficient τ is defined as the ratio between the power flow from room 1 to room 2 through the panel and the incident sound power on the wall in room 1, and is computed from the so-called coupling loss factor η_{12} between the rooms. Although the sound transmission loss results to be a random quantity (as the sound fields in the rooms are random diffuse fields), only its mean (i.e., ensemble averaged) value will be of interest in order to predict the

mean sound insulation of the panel. The mean sound transmission loss will depend on the frequency and on the panel properties, i.e. its geometry, size and material.

The sound transmission loss of the optimized layouts is shown in Figures 5 and 6, for PMMA and glazing panels respectively. Also, we show a comparison with reference uniform layouts that have the same mass as the optimized one. For all the considered cases both the harmonic behaviour and averaged curves in 1/3-octave bands are shown.

In the plots we can clearly see how the modal behaviour of the panel around the disturbance frequency is suppressed in the optimized layouts, as resonance dips, associated with structural eigenfrequencies, are effectively pushed away from the disturbance. This introduces a flattening in the harmonic transmission loss curves for the targeted frequency ranges, with associated improvements in the sound transmission loss around 5-10 dB with respect to the dip values. A flattened transmission loss curve increases also the robustness of the configuration to possible uncertainties in system parameters associated with the disturbance frequency and/or with the features of the structure, i.e. it reduces the probability that the disturbance frequency matches a resonance dip.

An improvement in the sound transmission loss can be seen also when averaging the curves in 1/3-octave bands. This especially holds for PMMA panels: in this case the optimized plates show improvements around 7 dB at the frequencies of the disturbance, when compared with the corresponding uniform plates. This kind of improvement is still present also for glazing panels, but results to be quantitatively lower. We motivate this by considering that the resonance dips in the glazing are more pronounced than in the PMMA, but also less
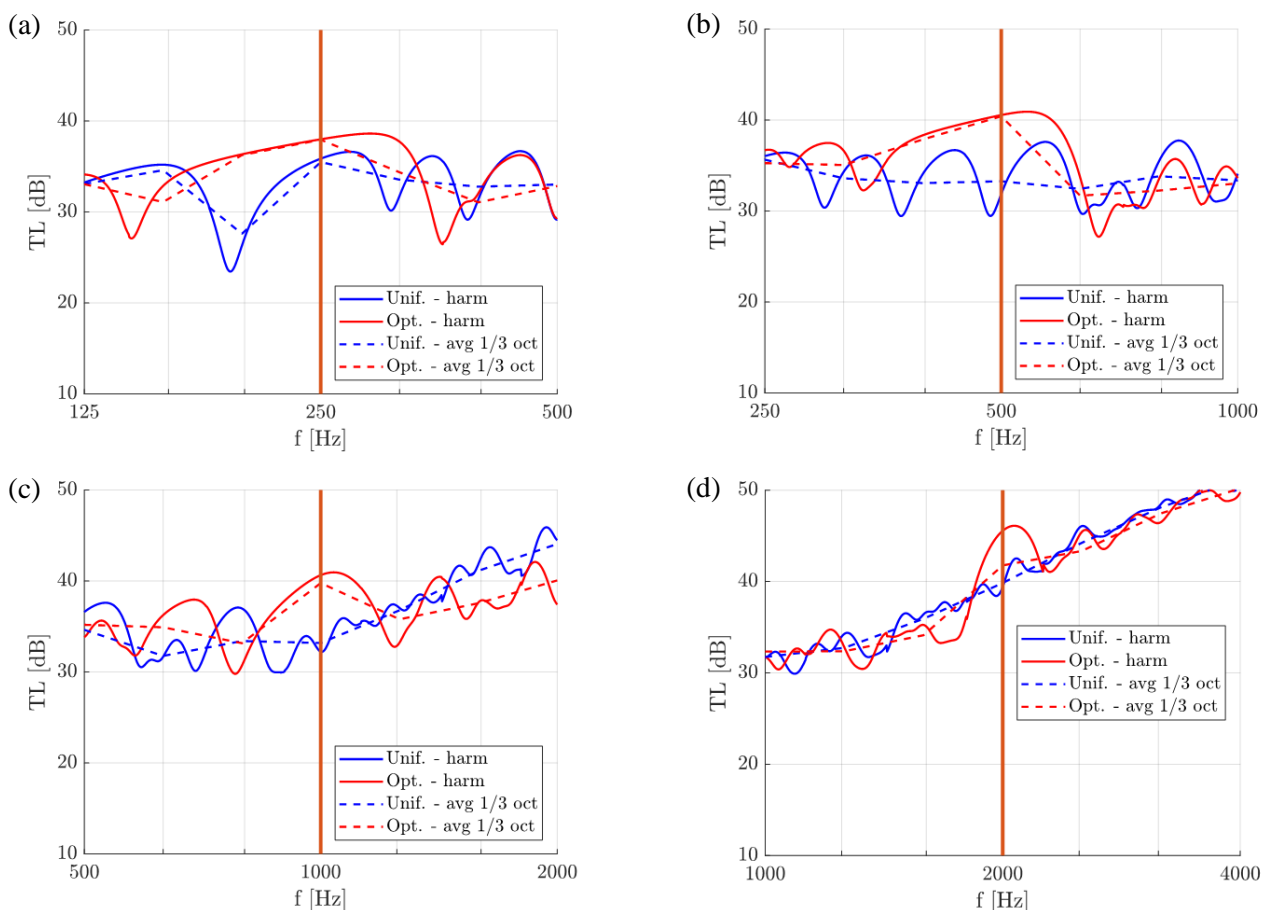
Figure 5 – Sound transmission loss curves for the PMMA layouts: (a) $f_c = 250$ Hz, (b) $f_c = 500$ Hz, (c) $f_c = 1000$ Hz, (d) $f_c = 2000$ Hz. Red curves refer to the optimized panels, while blue curves refer to uniform panels with the same mass as the optimized ones. Solid lines refer to harmonic plots, while dashed lines refer to averaging in 1/3-octave bands.
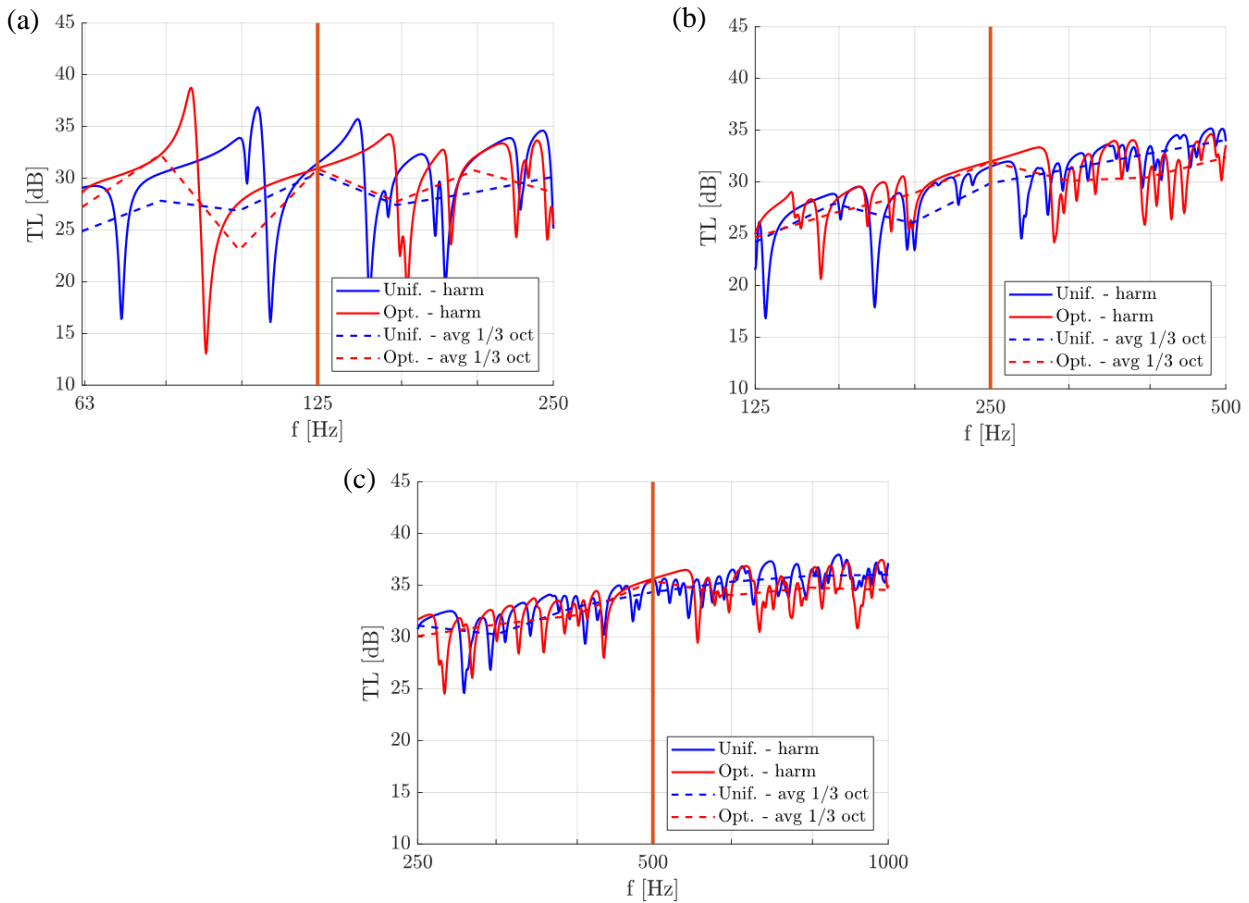
Figure 6 – Sound transmission loss curves for the glazing layouts: (a) $f_c = 125$ Hz, (b) $f_c = 250$ Hz, (c) $f_c = 500$ Hz. Red curves refer to the optimized panels, while blue curves refer to uniform panels with the same mass as the optimized ones. Solid lines refer to harmonic plots, while dashed lines refer to averaging in 1/3-octave bands.

wide in frequency, due to the low glazing damping properties (cf. Table 1). So we will have a different weight with respect to the PMMA when averaging the TL within 1/3-octave bands. Also, the admissible thickness range for the PMMA is bigger than the one for glazing, as for PMMA $t_{max} = 4 \cdot t_{min}$ and for glazing $t_{max} = 3 \cdot t_{min}$.

6 Conclusions

In this paper, topology optimization has been applied to design PMMA and glazing single plate panels with improved vibroacoustic behaviour in specific frequency bands.

The material thickness distribution within the panel area has been optimized in order to maximize the width of the frequency range with no structural eigenfrequencies around a specific narrowband disturbance. The optimization has been carried out relying on an in-vacuo mechanical finite element model to compute the structural eigenfrequencies, that allows for a computationally efficient design procedure. The performance of the optimized panels in terms of sound transmission loss have been a posteriori verified through a finite element – statistical energy analysis (FE-SEA).

Different PMMA and glazing panels have been designed considering different target disturbance frequencies between 125 and 2000 Hz, obtaining at least a 1/3-octave band with no eigenfrequencies for all the considered design cases. The computation of the sound transmission loss shows how the proposed design methodology is

effective in suppressing the modal behaviour of the panel around the disturbance, achieving a good robustness of the configuration with respect to uncertainties in the system parameters. In particular, transmission loss improvements of at least 5-10 dB have been obtained with respect to the resonance dips observed in uniform panels with the same mass of the optimized ones.

The proposed approach can be extended towards the design of double plate panels, where the material distributions within each single leaf can be optimized to improve the modal behaviour of the fully coupled plate-cavity-plate system, and improve the associated vibroacoustic performance.

Acknowledgements

References

[1]   Li, Q., Wu, Q., Liu, J. et al. Topology optimization of vibrating structures with frequency band constraints. *Struct Multidisc Optim* 63, 1203–1218 (2021).

[2]   Van den Wyngaert, J., Schevenels, M., Reynders, E. Acoustic topology optimization of the material distribution on a simply supported plate. *Proceedings of the 23rd International Congress on Acoustics, ICA 2019*, 1208 – 1215 (2019).

[3]   Bendsoe M.P., Sigmund O., *Topology Optimization*, Vol. 95, Springer Berlin Heidelberg, Berlin, Heidelberg, 2004.

[4]   Reynders, E., Langley, R., Dijckmans, A., & Vermeir, G. A hybrid finite element - Statistical energy analysis approach to robust sound transmission modeling. *Journal of Sound and Vibration*, 333(19), 4621-4636, 2014.

[5]   Wang F., Lazarov B.S., Sigmund O. On projection methods, convergence and robust formulations in topology optimization. *Struct Multidiscip Optim* 43(6):767–784(2011).

[6]   Svanberg, K., The method of moving asymptotes—a new method for structural optimization. *Int. J. Numer. Meth. Engng.*, 24: 359-373 (1987).

[7]   Shorter P.J., Langley R.S., Vibro-acoustic analysis of complex systems, *Journal of Sound and Vibration*, 288 (3), 2005.

[8]   Shorter P.J., Langley R.S., On the reciprocity relationship between direct field radiation and diffuse reverberant loading. *J Acoust Soc Am.* 117(1):85-95, 2005.

[9]   Decraene C., Dijckmans A., Reynders E., Fast mean and variance computation of the diffuse sound transmission through finite-sized thick and layered wall and floor systems, *Journal of Sound and Vibration*, Volume 422, 2018, Pages 131-145 (2018).

[10] Reynders E., Van Hoorickx C., Dijckmans A., Sound transmission through finite rib-stiffened and orthotropic plates, *Acta Acustica united with Acustica*, Volume 102, Number 6, pp. 999-1010(12), 2016.